DOI: 10.1002/ange.201206301

Molecular Electronics

Quantum Soldering of Individual Quantum Dots**

Xavier Roy, Christine L. Schenck, Seokhoon Ahn, Roger A. Lalancette, Latha Venkataraman, Colin Nuckolls,* and Michael L. Steigerwald**

Here we describe a precise method to make electrical contact to an individual quantum dot (QD). This supramolecular construction connects the QD to its macroscopic environment, yet it does not disturb the nanoscopic quantum mechanical confinement of the excitons in these small solids. Quantum mechanical confinement has given rise to the hallmark optical properties of QDs,[1–3] but it has been of only limited use in electronic and opto-electronic applications[3] of QDs because of three interrelated problems: 1) the lack of knowledge of how to make innocent electrical contact to QDs; 2) the challenge of synthesizing atomically precise QDs; and 3) not having the methods to efficiently wire individual QDs in electrical devices. Robust electrical contact to the core of QDs is essential in the development of QD-based electronic devices[3–8] and for the extraction of hot electrons[9] and the separation of charges from multiple exciton states[10,11] in QD solar cells but yet it has only been thoroughly explored in the context of thin films and bulk samples of QDs[12–17] where function cannot be related to the poorly characterized structure and quantum confinement is compromised at best. Here we synthesize, for the first time, a molecularly discrete, crystallographically defined, electron-rich, metal chalcogenide cluster, Co_6Se_8,[18] that is capped with conjugated, molecular connectors that can couple electronically to nanoscale electrodes. We show that these connectors provide a well-defined electronic pathway for the transport of charge carriers through a single QD. We measure the conductance of individual QDs using a scanning tunneling microscope based break-junction (STM-BJ) technique[19–21] and compare our results with density functional theory.

Finally, we show that we can control the electronic coupling between the core of the QD and the conducting backbone of the connector by varying the connector structure allowing us to differentiate between conductive molecular connectors and insulating ones. These results establish quantum mechanical design rules for controlling the electronic coupling to a QD for the creation of QD-based electrical circuits.

The solid-state compound CoSe is an infrared bandgap semiconductor.[22] We synthesized a series of atomically precise cobalt selenide quantum dots[18,23,24] decorated with different molecular connectors (L2–L5). Connectors L2–L4 have a phosphine end that coordinates to the cobalt atom in the cluster and a thiomethyl end that is aurophilic. Connector L5 lacks a thiomethyl group and serves as a control. We selected this family of compounds based on the parent QD $Co_6Se_8(PEt_3)_6$ (**1**) (Figure 1 b) because its electron-rich core is a reservoir of carriers, and its synthesis is amenable to a broad range of phosphines. Single-crystal X-ray diffraction (SCXRD) shows that the Co_6Se_8 core of the clusters, **1**–**5**, are isostructural (Figure 2), forming an octahedron of Co atoms concentric with a cube of Se atoms. Cluster **4** packs with its six molecular connectors grouped into two diametrically opposed groups of three, resulting in an ideal conformation for bridging a linear gap between two electrodes, as illustrated in Figure 1 a.

We measured the conductance of both the individual QDs **2**–**5**, and the free connectors, L2–L5 using a scanning tunneling microscope based break-junction (STM-BJ) technique.[19] STM-BJ measurements use a gold tip and gold substrate to repeatedly form and break gold point contacts in solutions of the target compounds in 1,2,4-trichlorobenzene as solvent. Clusters **2**–**4** can bind to the Au electrodes through thiomethyl groups[25] whereas **5**, which lacks thiomethyl groups, cannot. The conductance across the Au gap is measured versus the tip/substrate separation at an applied voltage of 500 and 750 mV for L2–L5 and **2**–**5**, respectively. In the inset of Figure 3 a and b, we show sample traces measured for **2**, **4**, L2, and L4. These conductance traces show plateaus with lengths and conductance that characterize each compound, indicating that each forms junctions.

We created one-dimensional (1D) conductance and two-dimensional (2D) conductance–displacement histograms from the conductance traces.[21] Figure 3 a and b show 1D

[*] Dr. X. Roy, C. L. Schenck, Dr. S. Ahn, Prof. C. Nuckolls, Dr. M. L. Steigerwald
Department of Chemistry, Columbia University
New York, NY 10027 (USA)
E-mail: cn37@columbia.edu
mls2064@columbia.edu
Homepage: http://nuckolls.chem.columbia.edu/
Prof. R. A. Lalancette
Department of Chemistry, Rutgers State University
Newark, NJ 07102 (USA)
Prof. L. Venkataraman
Department of Applied Physics and Applied Mathematics
Columbia University, New York, NY 10027 (USA)
E-mail: lv2117@columbia.edu

[**] This work was supported primarily through the Center for Re-Defining Photovoltaic Efficiency Through Molecular-Scale Control, an Energy Frontier Research Center (EFRC) funded by the U.S. Department of Energy (DOE), Office of Science, Office of Basic Energy Sciences under award number DE-SC0001085. L.V. thanks the Packard Foundation for support. X.R. thanks the Natural Sciences and Engineering Research Council of Canada for a post-doctoral fellowship. C.L.S. is supported by the National Science Foundation Graduate Research Fellowship under award number DGE-1144155. We thank Brian Capozzi for help with the STM-BJ measurements.

Supporting information for this article is available on the WWW under http://dx.doi.org/10.1002/anie.201206301.

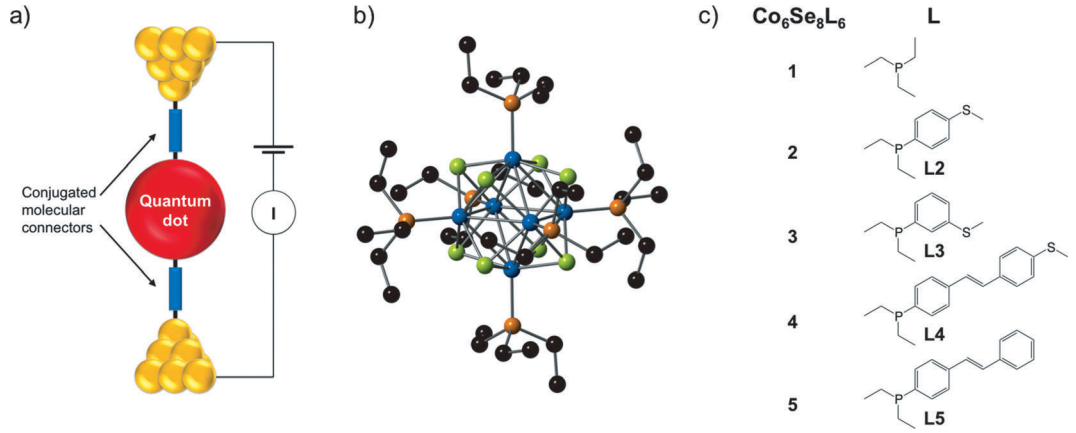

Figure 1. Making electrical contact to an atomically precise QD. a) Schematic of a single-cluster junction formed between nanoscale electrodes and molecular connectors. b) Molecular structure of the parent cluster $Co_6Se_8(PEt_3)_6$ (**1**). Carbon, black; cobalt, blue; phosphorus, orange; selenium, green. c) Chemical structures of the different ligand investigated in this study.

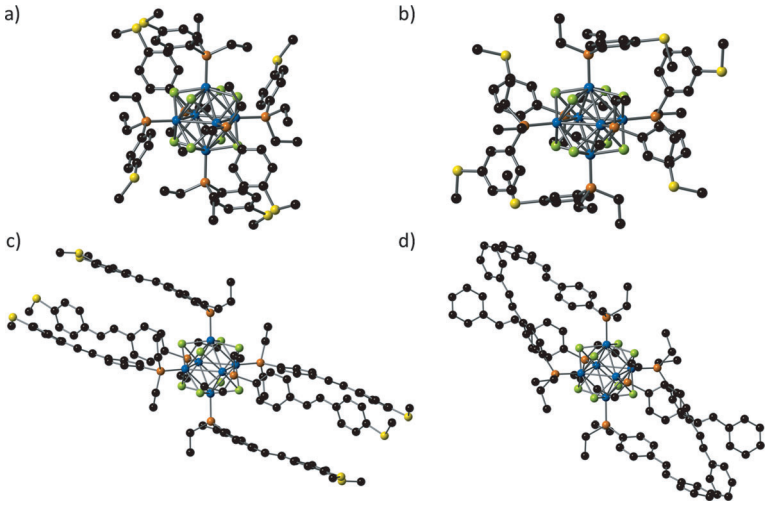

Figure 2. SCXRD characterization of the clusters. a–d) Molecular structures of clusters **2**–**5**, respectively. The hydrogen atoms and solvent molecules of crystallization have been omitted. Carbon, black; cobalt, blue; phosphorus, orange; sulfur, yellow; selenium, green. The Co-P, Co-Se, and Co-Co bond lengths for clusters **1**–**5** are in the range of 2.12–2.14 Å, 2.32–2.36 Å, and 2.88–2.97 Å, respectively. These distances change little in a given cluster and throughout the cluster series. The methyl group on one of the sulfur atoms in cluster **4** is disordered between two orientations (the site-occupancy-factor is 0.75:0.25).

conductance histograms generated using logarithm bins for **2**, **4**, L2, and L4. The histograms for the clusters do not overlap those of the corresponding connectors confirming that stable cluster junctions indeed form with **2** and **4**. The lower conductance of **2** and **4**, when compared with that of L2 and L4 is consistent with longer molecules spanning the junctions. The heights of the conductance peak for the clusters decrease after measurement of several thousand traces, possibly because of degradation under ambient conditions.

The 2D conductance–displacement histograms for **2** and **4**, shown in Figure 3c and d, extend to about 0.7 and 1.8 nm, respectively. This is significantly longer than for the corresponding connectors (2D histograms for L2 and L4 are shown in the Supporting Information in Figure S1) and agrees with previous measurements showing that longer molecules can bind further away from the apex of the Au electrodes and change their binding site on the electrode as the junctions are elongated.[21,26]

Cluster **5** lacks aurophilic thiomethyl functionality. Neither the 1D nor 2D conductance histograms for **5** (Figure S2 and S3) shows peaks as that of **4**. This suggests that cluster **4** forms molecular junctions by bonding its terminal thiomethyl groups to the Au electrodes, while **5** does not.

Comparison of **2** and **3** demonstrates the effect of the connector substitution pattern on the conductance of the cluster. Although the *meta*-substituted connector L3 shows a clear conductance peak that we ascribe to σ-conduction,[27–29] cluster **3** shows no peak (Figure S2). This indicates that no end-to-end electronic pathway exists in **3**. There is also no stepwise pathway by which a carrier can travel from one electrode to the cluster core and then to the second electrode. Thus when L3 binds to the cluster its 3-thiomethylphenyl substituent does not rotate around the P–C bond to enable conduction through a σ-pathway between the sulfur and the cluster core. These results show that we can effectively modulate the conductivity of a QD device by tuning the chemistry of the connectors by varying the substitution pattern or removing of the aurophilic group.

Electronic absorption spectroscopy, cyclic voltammetry, ^1H and ^{31}P NMR spectroscopies, and electronic structure calculations further characterize these molecular circuit elements. The absorption spectra (Figures S4–S8) show that modifying the connectors changes the Co_6Se_8 core little. The three longer-wavelength absorptions that characterize **1** remain essentially unchanged in **2**–**5**. The connectors L2–L5 absorb in the near-UV and **2**–**5** show similar absorptions. The spectra of the clusters are simply the sum of the spectra of the isolated constituent parts. This conclusion is supported by voltammetry of **2**–**5** (Figures S9–S12). Each cyclic voltammogram shows one reversible reduction and two reversible

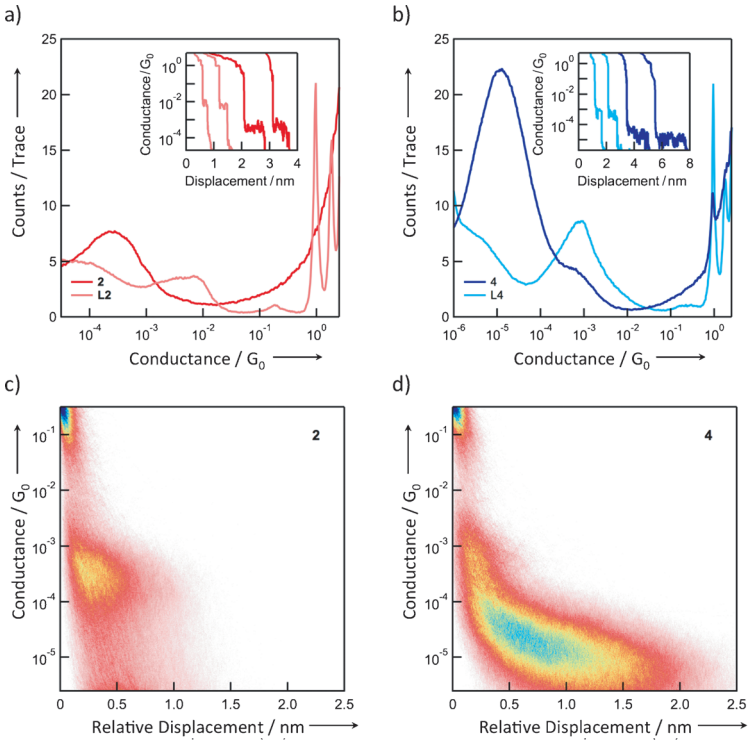

Figure 3. Single-cluster junctions. Logarithm-binned conductance histograms constructed using over 5000 traces for a) connector L2 (pink) and cluster **2** (red) and b) connector L4 (light blue) and cluster **4** (blue). The bin size is 100/decade. The insets show individual conductance traces. c and d) 2D conductance histograms for clusters **2** and **4**, respectively. The conductance peaks extend over a distance of 0.7 nm for **2** and 1.8 nm for **4** relative to the break of the gold point contact.

oxidations—identical behavior (and at essentially identical potentials) to **1**. We see no redox processes for the connectors on their own (L2–L5). Thus multiple charged states are reversibly accessible in **2**–**5**: the cluster core contains a number of stored charge carriers that can be transferred onto a macroscopic electrode. This voltammetry is complementary to the STM-BJ experiments that show the transport of charge carriers through conductive molecular connectors. The ^{1}H NMR spectra of **2**–**5** are essentially the same as for L2–L5. The single ^{31}P NMR resonance for **2**–**5** is significantly broader than and is shifted downfield from that of L2–L5, respectively, by about 75 ppm.

These data show that in most ways the clusters **1**–**5** are essentially identical; the differences in electronic absorption, chemical structure (determined both in the solid by SCXRD and in solution by NMR spectroscopy), and electronic structure (determined by cyclic voltammetry) are minor. In only two aspects do these clusters differ: **2** and **4** are electrically conductive, and they are much more sensitive to air than the others. For example, we can record sharp, well-defined ^{1}H NMR spectra for all of the clusters, but the spectra of **2** and **4** broaden rapidly after the samples are exposed to air while those of the other three clusters remain sharp. We suggest that these two features, molecular conductance and chemical reactivity, are two facets of the same fundamental property: access to the Co_6Se_8 core that is granted by L2 and L4 but forbidden by PEt_3, L3, and L5.

We and others have shown that 1,4-disubstitution on phenyl rings can give conductive, conjugated systems whereas compositionally similar 1,3-disubstitution gives insulating, cross-conjugated systems.[27–29] The present results extend this to include substituted phenyl phosphine ligands in metal-containing systems, and we use density functional theory to study this. We modeled **2**, **3** (Figure 4), and **4** (Figure S13) with the simpler clusters, $(PMe_3)_5Co_6Se_8(L2)$ and $(PMe_3)_5Co_6Se_8(L3)$, and $(PMe_3)_5Co_6Se_8(L4)$, respectively. The electronic structures of the three model clusters are very similar; the salient difference is in the orbitals that are most nearly identified with the pπ lone pairs on the sulfur atoms. Comparison of these orbitals in the model clusters indicates that the thiomethyl substituents are coupled more strongly to the cluster core in **2** and **4** than in **3**. We believe that the corresponding orbitals in **2** and **4** provide conduits through which electrons may move from the cluster to its ambient surroundings—either to effect electrical conduction in the break-junction or to mediate reaction with oxygen.

We supplemented these calculations with studies in which the Co_6Se_8 core was protected with four spectator PMe_3 ligands and two of the thiomethyl-containing ligands ($(PMe_3)_4Co_6Se_8(L)_2$) to characterize the electronic communication between antipodal aurophilic sites. We observe that the

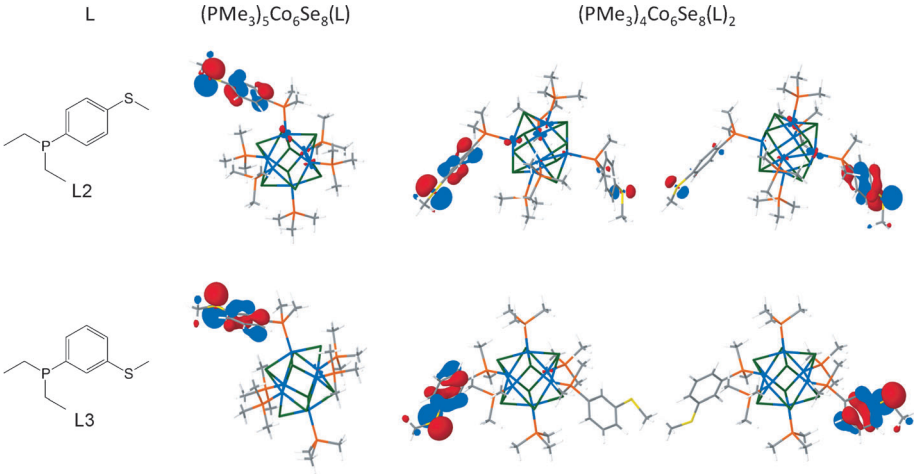

Figure 4. Model computational studies of clusters **2** and **3** using density functional theory. The orbitals associated with the sulfur pπ lone pairs for the models $(PMe_3)_5Co_6Se_8(L2)$, $(PMe_3)_5Co_6Se_8(L3)$, $(PMe_3)_4Co_6Se_8(L2)_2$, and $(PMe_3)_4Co_6Se_8(L3)_2$ are shown.

essential electronic structure of the cluster is unchanged; the significant differences again appear in the orbitals most readily associated with the sulfur pπ lone pairs (and also the C=C bond in the case of L4). We find that there is a clear, single-orbital pathway between the two antipodal points in $(PMe_3)_4Co_6Se_8(L2)_2$ and $(PMe_3)_4Co_6Se_8(L4)_2$ that is absent in $(PMe_3)_4Co_6Se_8(L3)_2$. These results are consistent with our experimental observations that **2** and **4** are electrically conductive and air-sensitive.

The compound $Co_6Se_8(PEt_3)_6$ is part of a large and varied family of metal chalcogenide molecular clusters that includes Chevrel phase analogues such as $Cr_6Te_8(PEt_3)_6$,[30] $Mo_6S_8(PEt_3)_6$,[31,32] and $W_6S_8(PCy_3)_6$,[4,33] and larger compounds that contain tens to hundreds of metal atoms.[34] We anticipate that our approach will provide a route to integrating clusters with tunable optical, electronic, and magnetic properties into electrical circuits and devices.

Quantum dots can act as reservoirs of electrical carriers or electronic excitations but this is valuable only to the extent that the charge or excitation can be removed from the cluster. In this study, we demonstrate a method to make contact and extract charge from one simple prototype. These results thus provide design rules for the preparation of structurally and electronically discrete quantum dots at molecular scale that reliably connect to nanoscale electrodes in a selective, well understood, and controllable fashion. Our work paves the way to incorporating these molecular electronic elements into circuits. We anticipate that this approach will be widely applicable to other quantum dot systems, thereby enabling a multitude of studies including the extraction of charges from multiple exciton states and extraction of hot carriers.

Received: August 6, 2012
Published online: November 7, 2012

Keywords: charge extraction · molecular wiring · quantum dots · scanning probe microscopy · single-molecule electronics

[1] M. G. Bawendi, M. L. Steigerwald, L. E. Brus, *Annu. Rev. Phys. Chem.* **1990**, *41*, 477 – 496.
[2] P. A. Alivisatos, *Science* **1996**, *271*, 933 – 937.
[3] D. V. Talapin, J.-S. Lee, M. V. Kovalenko, E. V. Shevchenko, *Chem. Rev.* **2010**, *110*, 389 – 458.
[4] M. Yuan, B. Ülgüt, M. McGuire, K. Takada, F. J. DiSalvo, S. Lee, H. Abruña, *Chem. Mater.* **2006**, *18*, 4296 – 4306.
[5] D. L. Klein, R. Roth, A. K. L. Lim, P. A. Alivisatos, P. L. McEuen, *Nature* **1997**, *389*, 699 – 701.
[6] M.-H. Jo, *Nano Lett.* **2006**, *6*, 2014 – 2020.
[7] D. I. Gittins, D. Bethell, D. J. Schiffrin, R. J. Nichols, *Nature* **2000**, *408*, 67 – 69.
[8] B. M. Boardman, J. R. Widawsky, Y. S. Park, C. L. Schenck, L. Venkataraman, M. L. Steigerwald, C. Nuckolls, *J. Am. Chem. Soc.* **2011**, *133*, 8455 – 8457.
[9] W. A. Tisdale, *Science* **2010**, *328*, 1543 – 1547.
[10] J. B. Sambur, T. Novet, B. A. Parkinson, *Science* **2010**, *330*, 63 – 66.
[11] A. J. Nozik, *Inorg. Chem.* **2005**, *44*, 6893 – 6899.
[12] D. V. Talapin, C. B. Murray, *Science* **2005**, *310*, 86 – 89.
[13] I. Robel, V. Subramanian, M. Kuno, P. V. Kamat, *J. Am. Chem. Soc.* **2006**, *128*, 2385 – 2393.
[14] S. Geyer, V. J. Porter, J. E. Halpert, T. S. Mentzel, M. A. Kastner, M. G. Bawendi, *Phys. Rev. B* **2010**, *82*, 155201.
[15] Y. Liu, M. Gibbs, J. Puthussery, S. Gaik, R. Ihly, H. W. Hillhouse, M. Law, *Nano Lett.* **2010**, *10*, 1960 – 1969.
[16] A. T. Fafarman, W.-k. Koh, B. T. Diroll, D. K. Kim, D.-K. Ko, S. J. Oh, X. Ye, V. Doan-Nguyen, M. R. Crump, D. C. Reifsnyder, C. B. Murray, C. R. Kagan, *J. Am. Chem. Soc.* **2011**, *133*, 15753 – 15761.
[17] T. P. Osedach, N. Zhao, T. L. Andrew, P. R. Brown, D. D. Wanger, D. B. Strasfeld, L.-Y. Change, M. G. Bawendi, V. Bulovic, *ACS Nano* **2012**, *6*, 3121 – 3127.
[18] S. M. Stuczynski, Y. U. Kwon, M. L. Steigerwald, *J. Organomet. Chem.* **1993**, *449*, 167 – 172.
[19] B. Q. Xu, N. J. J. Tao, *Science* **2003**, *301*, 1221 – 1223.
[20] A. Nitzan, M. A. Ratner, *Science* **2003**, *300*, 1384 – 1389.
[21] M. Kamenetska, M. Koentopp, A. C. Whalley, Y. S. Pakr, M. L. Steigerwald, C. Nuckolls, M. S. Hybertsen, L. Venkataraman, *Phys. Rev. Lett.* **2009**, *102*, 126803.
[22] W. Maneeprakorn, M. A. Malik, P. O'Brien, *J. Mater. Chem.* **2010**, *20*, 2329 – 2335.
[23] M. L. Steigerwald, *Polyhedron* **1994**, *13*, 1245 – 1252.
[24] M. L. Steigerwald, T. Siegrist, S. M. Stuczynski, *Inorg. Chem.* **1991**, *30*, 4940 – 4945.
[25] Y. S. Park, A. C. Whalley, M. Kamenetska, M. L. Steigerwald, M. S. Hybertsen, C. Nuckolls, L. Venkataraman, *J. Am. Chem. Soc.* **2007**, *129*, 15768 – 15769.
[26] J. S. Meisner, M. Kamenetska, M. Krikorian, M. L. Steigerwald, L. Venkataraman, C. Nuckolls, *Nano Lett.* **2011**, *11*, 1575 – 1579.
[27] S.-H. Ke, W. Yang, H. U. Baranger, *Nano Lett.* **2008**, *8*, 3257 – 3261.
[28] D. M. Cardamone, C. A. Stafford, S. Mazumdar, *Nano Lett.* **2006**, *6*, 2422 – 2426.
[29] S. V. Aradhya, J. S. Meisner, M. Krikorian, S. Ahn, R. Parameswaran, M. L. Steigerwald, C. Nuckolls, L. Venkataraman, *Nano Lett.* **2012**, *12*, 1643 – 1647.
[30] B. Hessen, T. Siegrist, T. Palstra, S. M. Tanzler, M. L. Steigerwald, *Inorg. Chem.* **1993**, *32*, 5165 – 5169.
[31] T. Saito, N. Yamamoto, T. Yamagata, H. Imoto, *J. Am. Chem. Soc.* **1988**, *110*, 1646 – 1647.
[32] S. Jin, F. Popp, S. W. Boettcher, M. Yuan, C. M. Oertel, F. J. DiSalvo, *J. Chem. Soc. Dalton Trans.* **2002**, 3096 – 3100.
[33] S. Jin, D. Venkataraman, F. J. DiSalvo, *Inorg. Chem.* **2000**, *39*, 2747 – 2757.
[34] J. F. Corrigan, O. Fuhr, D. Fenske, *Adv. Mater.* **2009**, *21*, 1867 – 1871.